



Atorvastatin treatment softens human red blood cells: an optical tweezers study

VAHID SHEIKH-HASANI,¹ MEHRAD BABAEI,^{1,5} ALI AZADBAKHT,^{2,5}
HAMIDREZA PAZOKI-TOROUDI,³ ALIREZA MASHAGHI,⁴ ALI AKBAR
MOOSAVI-MOVAHEDI,^{1,6} AND SEYED NADER SEYED REIHANI^{2,7}

¹*Institute of Biochemistry and Biophysics, University of Tehran, Tehran, Iran*

²*Department of Physics, Sharif University of Technology, Tehran, Iran*

³*Physiology Research Center and Department of Physiology, Faculty of Medicine, Iran University of Medical Sciences, Tehran, Iran*

⁴*Leiden Academic Centre for Drug Research, Faculty of Science, Leiden University, Leiden, The Netherlands*

⁵*These authors contributed equally to this work.*

⁶*moosavi@ut.ac.ir*

⁷*sreihani@sharif.edu*

Abstract: Optical tweezers are proven indispensable single-cell micro-manipulation and mechanical phenotyping tools. In this study, we have used optical tweezers for measuring the viscoelastic properties of human red blood cells (RBCs). Comparison of the viscoelastic features of the healthy fresh and atorvastatin treated cells revealed that the drug softens the cells. Using a simple modeling approach, we proposed a molecular model that explains the drug-induced softening of the RBC membrane. Our results suggest that direct interactions between the drug and cytoskeletal components underlie the drug-induced softening of the cells.

© 2018 Optical Society of America under the terms of the [OSA Open Access Publishing Agreement](#)

OCIS codes: (350.4855) Optical tweezers or optical manipulation; (170.4520) Optical confinement and manipulation; (000.1430) Biology and medicine; (170.1420) Biology.

References and links

1. O. K. Baskurt, and H. J. Meiselman, "Blood Rheology and Hemodynamics," *Semin. Thromb. Hemost.* **29**, 435–450 (2003).
2. S. Suresh, "Mechanical response of human red blood cells in health and disease: Some structure-property-function relationships," *J. Mater. Res.* **21**, 1871–1877 (2006).
3. S. Hénon, G. Lenormand, A. Richert, and F. Gallet, "A new determination of the shear modulus of the human erythrocyte membrane using optical tweezers," *Biophys. J.* **76**, 1145–1151 (1999).
4. Y. Z. Yoon, J. Kotar, G. Yoon, and P. Cicutta, "The nonlinear mechanical response of the red blood cell," *Phys. Biol.* **5**, 36007 (2008).
5. F. R. Maxfield, and I. Tabas, "Role of cholesterol and lipid organization in disease," *Nature* **438**, 612–621 (2005).
6. G. G. Schwartz, "Effects of Atorvastatin on Early Recurrent Ischemic Events in Acute Coronary Syndromes," *JAMA* **285**, 1711–1718 (2001).
7. A. M. Forsyth, S. Braunmüller, J. Wan, T. Franke, and H. A. Stone, "The effects of membrane cholesterol and simvastatin on red blood cell deformability and ATP release," *Microvasc. Res.* **83**, 347–351 (2012).
8. G. M. Morris, R. Huey, W. Lindstrom, M. F. Sanner, R. K. Belew, D. S. Goodsell, and A. J. Olson, "AutoDock4 and AutoDockTools4: Automated docking with selective receptor flexibility," *J. Comput. Chem.* **30**, 2785–2791 (2009).
9. M. F. Sanner, "Python: a programming language for software integration and development," *J. Mol. Graph. Model.* **17**, 57–61 (1999).
10. A. W. Schüttelkopf and D. M. F. van Aalten, "PRODRG : a tool for high-throughput crystallography of protein-ligand complexes," *Acta Crystallogr. Sect. D Biol. Crystallogr.* **60**, 1355–1363 (2004).
11. V. B. Chen, W. B. Arendall, J. J. Headd, D. A. Keedy, R. M. Immormino, G. J. Kapral, L. W. Murray, J. S. Richardson, and D. C. Richardson, "MolProbity : all-atom structure validation for macromolecular crystallography," *Acta Crystallogr. Sect. D Biol. Crystallogr.* **66**, 12–21 (2010).
12. D. A. Fletcher and R. D. Mullins, "Cell mechanics and the cytoskeleton," *Nature* **463**, 485–492 (2010).
13. T. Betz, M. Lenz, J.-F. Joanny, and C. Sykes, "ATP-dependent mechanics of red blood cells," *Proc. Natl. Acad. Sci.* **106**, 15320–15325 (2009).

14. J. Sleep, D. Wilson, R. Simmons, and W. Gratzel, "Elasticity of the Red Cell Membrane and Its Relation to Hemolytic Disorders: An Optical Tweezers Study," *Biophys. J.* **77**, 3085–3095 (1999).
15. J. Greenwood, L. Steinman, and S. S. Zamvil, "Statin therapy and autoimmune disease: from protein prenylation to immunomodulation," *Nat. Rev. Immunol.* **6**, 358–370 (2006).
16. G. J. Blake, and P. M. Ridker, "Are statins anti-inflammatory?" *Curr Control Trials Cardiovasc Med* **1**, 161–165 (2000).
17. M. Russo, M. Scobey, and H. Bonkovsky, "Drug-Induced Liver Injury Associated with Statins," *Semin. Liver Dis.* **29**, 412–422 (2009).
18. B. A. Parker, and P. D. Thompson, "Effect of Statins on Skeletal Muscle," *Exerc. Sport Sci. Rev.* **40**, 1–12 (2012).

1. Introduction

Blood plays a vital role in maintaining physiological homeostasis in the human body. This non-newtonian colloidal liquid can transport a large number of species, such as respiratory gasses, nutrients and drugs, all over the entire body. It is believed that rheological behavior of this compound fluid is in close relation with its function [1]. For instance, physical deformation of the Red Blood Cells (RBCs) underlies pathological manifestations of sickle cell anemia and hypercholesterolemia. Therefore, one can expect a correlation between the physical properties of RBC and the state of overall health of the cell [2]. In this regards a large scientific effort is focussed on mechanical properties of RBC [2–4].

Cholesterol content of RBC membrane is a major determinant of RBC mechanics and is significantly altered in hypercholesterolemia, a disorder that dramatically increases the risk of developing cardiovascular diseases [5]. Cholesterol plays a crucial role in structural integrity and functioning of the membrane of the RBCs. An increase or decrease in the level of membrane cholesterol could alter vital processes such as membrane trafficking, cell signaling as well as membrane phase behaviour [5]. Statins-family of drugs are commonly prescribed for hypercholesterolemia patients with both primary and secondary prevention in order to decrease the level of the blood cholesterol. Statin drugs, thus affect RBC mechanics indirectly through modulation of cholesterol content of the membrane [6]. It is however unclear whether statin drug can directly affect RBC mechanics, or more broadly, mechanics of human cells.

In this article, we ask whether statin drugs directly affect mechanical properties of human RBCs or not. We study Atorvastatin, a commonly prescribed statin drug, and show that it can affect the mechanical properties of human RBC. We compare the viscoelastic properties of healthy and Atorvastatin-treated RBC at single-cell level using Optical Tweezers (OT). OT are commonly used for single-cell mechanical studies due to their better resolution for piconewton range forces. we propose a mechanism that explains the observed softening. This is achieved by performing molecular modeling analysis of the interactions between Atorvastatin and RBC membrane. Our results reveal molecular interactions between drug and cytoskeleton proteins. We find that Atorvastatin induces protein conformational changes that may lead to a significant increase in the flexibility of the cell.

2. Material and methods

2.1. Sample preparation

All samples were prepared using sterile normal saline (PSS) containing 9 mg/ml NaCl solution. Blood samples were first taken from healthy volunteers using sterile finger picks and then diluted in PSS, after which were incubated with the drug solution for about 10 minutes. In order to prepare the drug solution, first, a small amount of the drug was dissolved in PSS by sonication at 37°C for 60 minutes. After flushing the solution through a 0.25 μ m filter the final concentration of the drug solution was set to 0.7 μ g/ml [7].

2.2. Optical micromanipulation setup

Our OT setup consists of a CW laser source (Nd:YAG, $\lambda=1064\text{nm}$, Coherent) implemented in a home-designed inverted microscope. The collimated laser beam is focused using a high Numerical Aperture (NA) objective lens (UPlanSApo, 60 \times , NA=1.20, Water, Olympus). The sample chamber holder is mounted on a piezo stage (P-753.21C, Physik Instrumente). This allows for spatial nano-positioning of the trap inside the sample chamber. A Quadrant Photo Diode (QPD) positioned at the back focal plane of the condenser allows for measuring the displacements of the trapped bead from the center of the trap with nanometer spatial and megahertz temporal resolutions. In a typical measurement the RBC of interest was firmly attached to two separate polystyrene beads from its diagonal sides, as it is schematically shown in the inset of Fig. 1(b). In the final experimental assay the large bead ($\sim 4\mu\text{m}$, Anti-dig polystyrene, Kisker Biotech) was attached to the glass chamber wall using van der Waals interaction, whereas the small bead ($\sim 2\mu\text{m}$, Anti-dig polystyrene, Kisker Biotech) was optically trapped. The attachment of the beads to the cell's membrane was done by conjugation of the anti-dig (on the bead's surface) and the cell's surface proteins with carbohydrate residues (including Band-3 protein). It should be mentioned that before attaching the small bead to the cell the trap was calibrated. In order to do that, first, the voltages of the QPD were recorded for three seconds at a sampling rate of 22kHz. The trap stiffness and the voltage-to-position conversion factor were obtained by power spectrum analysis of the recorded time series. It is worth mentioning that the size of the trapped bead was chosen so that the cell was not directly exposed to the laser beam, even in the most displaced position.

2.3. Manipulation cycle

The entire measurement was conducted in a cyclic manner, in which the cell is periodically subjected to an external tensile force followed by a relaxation time. More specifically, the manipulation cycle consisted of four separate steps as follows: Step 1 (stretch): the cell was stretched with a pre-known strain rate. This was done by translating the sample chamber with a pre-known velocity for $2\mu\text{m}$. Due to its viscoelastic nature, the cell may show a wide range of stiffnesses for this step depending on the velocity that it is pulled out. Step 2 (relax): The stage was kept stationary for over 20 seconds. In this step the cell is given a time to relax the exerted tension and come to a mechanical equilibrium. Step 3: The sample chamber was moved back by $2\mu\text{m}$ at the same velocity used in step 1. Step 4: The sample chamber was kept stationary for over 20 seconds in order to let the RBC relax, again. During the entire process the force experienced by the trapped bead was monitored at a sampling rate of 5kHz. Typical force-time and force-displacement graphs for a Healthy-Fresh (HF) and Drug-Treated (DT) RBCs are shown in Fig. 1(a) and 1(b), respectively.

2.4. Molecular docking

Molecular docking was carried out using Autodock suit version 4.3 [8] and MGL tools version 1.5.6 [9] with standard parameters. The molecular structure of Atorvastatin was created and energy minimized using PRODRG2 online server [10]. The molecular structure of the spectrin-binding domain of ankyrin and F-actin were obtained from the protein data bank with PDB codes of 3KBT and 3J8A, respectively. The proteins' structure were checked for missing atoms and any possible bad contacts and clashes was fixed using Molprobit online server [11].

3. Results and discussion

In order to compare the viscoelastic properties of HF and DT cells the manipulation cycle was repeated on the two cell types. In the following, different aspects of the response graphs will be discussed. The results are based on 26 HF and 17 DT manipulation cycles.

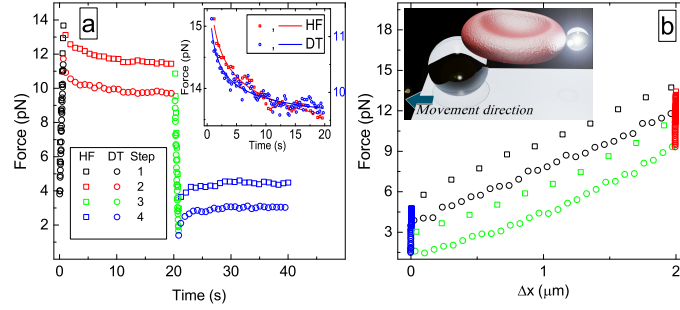


Fig. 1. The measured force as a function of: (a) time, and (b) elongation in a typical manipulation cycle. Each step is shown using a separate color code to be distinguishable. Inset: (a) The relaxation data for the healthy-fresh (red squares) and drug-treated (red circles) of the main graph are fitted to a power law decay function (equation 1).

3.1. Stress relaxation study

Typical relaxation graphs for the Healthy-Fresh (HF) and Drug-Treated (DT) cells are shown in the inset of Fig. 1. This relaxation is mainly due to the rearrangement of cytoskeletal network in response to the external tensile stress [12]. The previous studies have shown that during this relaxation the holding force can be expressed using a power-law decay function [2]. Therefore, the recorded relaxation data were fitted to the following function [4]

$$F(t) = \Delta F_0 \times \left(\frac{t}{t_0}\right)^{-\alpha_f} + F_{inf} \quad (1)$$

where $F(t)$, ΔF_0 , α_f , and F_{inf} denote the measured force at time t , final force value (corresponding to the plateau), relaxation time constant, and a constant, respectively. In order to use dimensionless time, t_0 was set to 1s. Note that the value of α_f obtained in this step is independent of the strain rate used in step 1. Fitting the relaxation graphs to equation 1 (Fig. 1(a)-inset) resulted in α_f of 0.25 ± 0.03 and 0.34 ± 0.03 , respectively, for the HF and DT cells. It is previously shown that an ATP dependent internal metabolism could alter the relaxation power, α_f [13]. Therefore, one possible reason for the slight difference in the α_f values of the two cell types could be that the metabolism pathway and re-association of the protein network is being altered by the drug molecules attached to the cytoskeletal proteins. As it can be seen from molecular docking results relatively strong binding of Atorvastatin to two important cytoskeletal junctions would be a possible reason for alteration of cytoskeleton re-association. It is worth mentioning that at the strain rates used in this research (step 1 of the cycles) though the initial force of the relaxation graph could be different, however, the resulted values for α_f were the same within the error bars.

3.2. Dynamic stiffness study

As mentioned earlier, the cell is pulled out at a constant strain rate in step 1 of the manipulation cycle. Therefore, the dynamic stiffness of the cell can be obtained from the slope of the force-elongation graph (black symbols in Fig. 1(b)). In order to determine the dependency of the dynamic stiffness on the strain rate, the manipulation cycle was repeated at different strain rates, the results of which are summarized in Fig. 2(a). It is shown that the dynamic stiffness of the cell should be a power-law function of the strain rate as below [4]

$$K(\dot{\epsilon}) = \Delta K(\dot{\epsilon}) + K_0 = \Delta K_0 \times \left(\frac{\dot{\epsilon}}{\dot{\epsilon}_0}\right)^{-\alpha_k} + K_0 \quad (2)$$

where k_0 and α_k , respectively, denote the stiffness at $\dot{\epsilon}=0 \text{ s}^{-1}$, and the power factor. Note that K_0 (can be considered as stationary stiffness) should be independent of the strain rate. By fitting the

dynamic stiffness graphs to Eq. (2) we obtained α_k of 0.39 ± 0.04 and 0.54 ± 0.03 , respectively, for the HF and DT cells. Note that the power factor resulted for the HF cell is in good agreement with the previous reports [14], and that the lower k_0 of the DT cells is accompanied by a larger power factor compared to the HF cells. In other words though the DT cells seem softer at zero strain rate, however, their stiffness grows faster when the strain rate is increased. But, in all of the strain rates used in this research the DT cell seemed to be softer than the HF cells. The inset of Fig. 2(a) shows the histogram of the resulted stiffness at a strain rate of 0.37 s^{-1} . At this strain rate, the dynamic stiffness for the HF and DT cells, respectively, were $4.5 \pm 0.2 \text{ pN}/\mu\text{m}$ and $3.6 \pm 0.3 \text{ pN}/\mu\text{m}$, which reveals that the DT cells are softer by $\sim 25\%$. It should be mentioned that the histogram graphs were put under student T-test and the graphs are indeed distinguishable.

3.3. Dissipated energy study

The hysteresis-type behavior shown in Fig. 1(b) reveals that there is a dissipated energy in each cycle. The amount of the dissipated energy in each cycle can be estimated by the area inside the force-elongation graph (Fig. 1(b)). The larger the area the larger the dissipated energy. Fig 2(b) shows how the dissipated energy depend on the strain rate. It is theoretically shown that the dissipated energy should be a power-law decay function of the strain rate as below [4]

$$E_{dissp} = E_0 + E \left(\frac{\dot{\epsilon}}{\dot{\epsilon}_0} \right)^{\alpha_E} \quad (3)$$

The solid lines in Fig. 2(b) show fit to Eq. (3) with resulted power factors (α_E) of 0.63 ± 0.02 and 0.7 ± 0.01 , respectively, for the HF and DT cells.

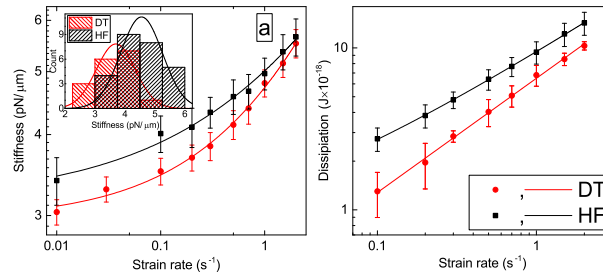


Fig. 2. Comparison of the HF and DT cells: (a) Dynamic stiffness as a function of strain rate. The solid lines are the fits to the power-law decay function (Eq. (2)). Inset: Histogram of the resulted stiffnesses for HF and DT cells at strain rate of 0.37 s^{-1} . (b) The dissipated energy as a function of the strain rate. The solid lines are fits to Eq. (3).

3.4. Molecular modeling

It is known that the total stiffness of the cell is mainly dominated by its spectrin network. Therefore, it is very likely that the observed softening in the cell occurs due to the interaction between the Atorvastatin molecule and the spectrin network of the cell. In order to test this hypothesis, a molecular docking study was carried out. In this study the spectrin-binding domain of the ankyrin and f-actin proteins were chosen as targets for the Atorvastatin molecule. Fig. 3 shows a 3-D visualization of the drug molecule next to the proteins, in which the spatial fitting of the molecule in the surface clefts are shown. The molecular docking results showed that Atorvastatin molecule has a large affinity to attach to either of the proteins due to the nearly perfect molecular shape-matching. Apart from the spatial geometry, the polarity complementarity may also assist this fitting. In order to see this more clearly in the figure, the non-polar, positively charged, and negatively charged residues are shown in white, blue, and red, respectively. Fig. 3 shows that the

polar tail of the Atorvastatin molecule has a good tendency to approach the positively charged polar regions in both of the proteins. Furthermore, the aromatic rings of the drug molecule may also be positioned in the non-polar cleft in both of the proteins. Besides, in both cases some hydrogen bonds are created between the drug molecule and the proteins. The above mentioned points further suggest that the drug molecules may be attached to the spectrin network of the cell, which could explain the observed softening of the cell upon Atorvastatin treatment. It was reported that proteolytic dissociation of spectrin-ankryne complex or extraction of actin junctions remarkably reduced stiffness of RBCs [14]. According to our results, in a similar way the drug binding could loosen the junctional proteins interaction and, therefore, reduce the stiffness of the RBCs.

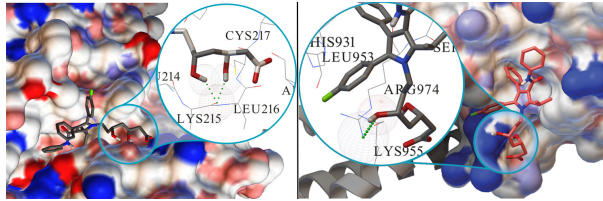


Fig. 3. Molecular docking results: Three dimensional surface map showing how a Atorvastatin molecule interacts with f-actin (left), and spectrin-binding-domain of ankryn (right).

4. Conclusion

Statin family of drugs are commonly used for prevention and treatment of several diseases, including cardiovascular diseases and cancer [15], yet cellular responses to statin drugs have not been fully investigated. In addition to its lipid lowering effect, several beneficial are observed for this drug family, including the anti-inflammatory effect [16], reduced isoprenylation of proteins, and inhibition of GTPases [15]. Moreover, several side effects have been reported for this drug family, including hepatotoxicity [17], rhabdomyolysis, and muscular problems [18]. Here, we studied the effects of a statin drug on cellular mechanics. More specifically, we studied the effects of atorvastatin on RBC mechanics. According to our experimental results the atorvastatin treated human red blood cells are softer than the healthy-fresh red blood cells. Our molecular docking results show that the atorvastatin molecule has a relatively high affinity to bind to the spectrin binding domain of ankyrin and F-actin proteins due to the shape and charge complementarity. Such a binding could alter the proteins conformation as it can change the strength of the native interactions in the junctions. This could even cause dissociation in some of the junctions in the cytoskeletal network leading to a total softening of the cell [14]. Further molecular investigation in this regard, such as all-atom molecular dynamics simulations, could reveal valuable information. It is known that the drugs designed for a specific treatment may also have some other side-effects. In some cases the side effect may even be considered as a possibility to use against another related (or even completely different) disease. This means that this drug may also be used against the RBC hardening diseases.

Funding

Sharif University of Technology (G930208); Iran National Science Foundation (INSF) (G95844788).

Disclosures

The authors declare that there are no conflicts of interest related to this article.